

Green synthesis of Ag Nanoparticles on Reduced Graphene

Oxide Nanocomposite and Promising Application for Dye

Removal

Author: Gowthamraj. V, Mphil (Chemistry)

Bharath Institute Of Higher Education And Research, Chennai 600 073

Email Id: menongowtham84@gmail.com

Guide: Dr. K. Rajendran, Associate Professor

Bharath Institute Of Higher Education And Research, Chennai 600 073

Email Id: rajendran1317@gmail.com

Address for Correspondence

Author: Gowthamraj. V, Mphil (Chemistry)

Bharath Institute Of Higher Education And Research, Chennai 600 073

Email Id: menongowtham84@gmail.com

Guide: Dr. K. Rajendran, Associate Professor

Bharath Institute Of Higher Education And Research, Chennai 600 073

Email Id: rajendran1317@gmail.com

ABSTRACT:

In this chapter, a facile green process was developed for the synthesis of AgNPs - rGO composite by using *Citrullus colocynthis* leaf extract as a reducing and stabilizing agent. The morphology and microstructure of the magnetic nanocomposite was examined by FTIR, XRD, UV-VISIBLE and SEM. Here, the green synthesized nanocomposite display remarkable effective removal of Methylene Blue (MB) from aqueous solution, showing a maximum adsorption capacity reached up to 146.43 mg L⁻¹ within only 30 minutes at room temperature. The kinetics, isotherms and thermodynamics of the adsorption of MB have been studied at various experimental conditions (initial dye concentration of MB, adsorbent dosage, contact time and temperature). Adsorption kinetics and the equilibrium adsorption isotherm were found to follow a pseudo-second order kinetic model and Langmuir isotherm, respectively. The thermodynamic parameters indicated that the adsorption was spontaneous, favorable, and endothermic in nature. Moreover, AgNPs - rGO was very stable and can be readily reuse by washing with water. Therefore we believed that the prepared nanocomposite as a very good green adsorbent for eliminating MB pollutant from aqueous solution.

Introduction

Nowadays, metal nanoparticles are gaining great interest in treatment of pollutants contaminated waste water. Particularly, Silver nanoparticles (AgNPs) have many promising applications in nanotechnology because of their good electrical conductivity, chemical stability, catalytic and antibacterial properties.[1] These properties depend mainly on their size, shape, composition, structure and morphologies[2]. biosensors[3], catalysts [4], and environment remediation [5]. Due to large specific surface area, high surface reactivity [6], high affinity [7] and low cost, AgNPs are promising adsorbent for environmental applications. It can be synthesized by various methods such as, vacuum sputtering [8], decomposition in organic solvents [9] and chemical reduction with sodium borohydride(NaBH₄)[10]. Generally, AgNPs produced by chemical reduction of Silver with NaBH₄ as a reducing agent is a routine synthesis reported so far. Stabilizers such as chitosan [11], activated carbon [12] and carboxymethyl cellulose [13] are commonly added in these reduction methods to synthesizestable, small size AgNPs. Among, these syntheses are generally expensive and require special equipment, high energy and involve chemical substances that are toxic, costly, corrosive and flammable, and non eco-friendly [14].To conquer this problem, nowadays a simple, cost effective and environmentally friendly new green reduction method being preferred. Compare to the other biological systems the plant materials make attractive platform for bioreduction due to low cost cultivation, short production time, safety and the ability to large scale production of AgNPs. Moreover, homogeneous AgNPs is undesirable for industrial and environmental application because of their number of drawbacks such as easy oxidation, rapid agglomeration, difficult in solid/liquid separation and adsorbent recycling become major challenges. In order to overcome these challenges, metal nanoparticles(MNPs) are generally anchored on sand [15], zeolite [16], clay[17] and carbon[18].

MATERIALS AND METHODS

Materials

Natural graphite powder, Methylene blue (MB) [C₁₆H₁₈N₃OS, MW: 333.6 g mol⁻¹, λ_{max}: 630 nm], sulfuric acid (H₂SO₄, 98%), hydrochloric acid (HCl, 37%),hydrogen

Research Paper

peroxide (H₂O₂), sodium nitrate (NaNO₃), potassium permanganate,(KMnO₄), Silver Nitrate(AgNO₃), were purchased from Sigma-Aldrich, India.*Citrullus colocynthis* leaf was collected from local area in Madurai, Tamil Nadu. All aqueous solutions used in this work were prepared by deionized water. All chemicals are analytical purity and were used without any further purification.

Synthesis of GO

Graphene oxide (GO) was synthesized from natural graphite powder by a modified Hummers method [39]. Briefly, 1g of graphite powder was added to the mixture of 0.5g of NaNO₃ and 25 mL H₂SO₄ into a 250 mL beaker following by 30 min stirring at 0^oC. Subsequently, 6 g of KMnO₄ was added slowly to the suspension with stirring. After stirring for 2 h, the temperature of the mixture was heated to 35^oC ± 5^oC for 30 min. 90 mL of water was slowly added and then the solution was further heated to 90^oC under vigorous stirring for 15 min. Then, 60 mL of H₂O₂ aqueous solution was added to the suspension until its color was changed from drab to brilliant yellow to reduce the residual MnO₂. The yellow graphite oxides were washed by diluted HCl (5%) and DI water three times to eliminate SO₄²⁻ and H⁺ respectively. Finally, the resulting solid was dried in a vacuum oven at 50^oC for 24h to get GO.

Preparation of aqueous *Citrullus colocynthis* leaf extracts (CCLE)

Locally collected fresh *Citrullus Colocynthis* leaves were cleaned. The aqueous extract was prepared by the addition of 20g of leaves with 100 mL distilled water at 80^oC for 5min. Further the extract was filtered and the filtrate was stored (10^oC) for further use.

Synthesis AgNPs-rGO composite.

AgNPs-rGO composites were synthesized by green method. The synthesis methods of AgNPs-rGO composite were carried out as follows: AgNO₃ (in 50ml) solution was mixed into the GO aqueous solution (10ml, 0.1mg/1ml). The mixture was magnetically stirred for 10 mins to form homogeneous solution. Then, 60ml of freshly prepared aqueous CCLE was added drop wise into the above solution followed by further stirring for 30 min at 60^oC. The resulting suspension was centrifuged for 10 min and washed with water for several times to get free of excess chemicals. Finally the residue was dried at 50^oC to yield AgNPs-rGO

Research Paper

composites. Similar procedures were used to synthesize of AgNPs was also carried out without GO using the same experimental conditions.

Preparation of Stock Solution

The MB stock solution of 500 ppm concentration was prepared by dissolving an accurately weighted amount of MB in DI water. The desired concentrations of the solution were obtained by diluting the stock of MB solution in exact proportions to obtain different initial concentrations.

Adsorption Experiments

Adsorption of MB onto the AgNPs-rGO composite was investigated by a batch method. Batch adsorption experiments have been performed by mixing 50 mL of a dye solution (250 ppm to 500 ppm of concentration) with 5 mg to 30 mg of the AgNPs-rGO composite in 250 ml iodine flask at stirring rate 120 rpm.

Sample flasks were shaken on a shaker and operated at a constant temperature of 35°C and 120 rpm for 1 h. Finally, 5 mL of sample was continuously taken for adsorption analysis at appropriate time intervals (0, 6, 12, 18, 24, 30 and 60 min) and the adsorbed amount of dyes was calculated by Beer's law. Then, dye solutions were separated from the mixture by centrifuge (12000 rpm for 20 min) and analyzed

by UV–vis spectroscopy. Concentration of the dye solution was determined

colorimetrically by measuring at maximum absorbance of the MB dye ($\lambda_{\max} = 663 \text{ nm}$).

Preliminary experiments indicated that the adsorption of MB reached equilibrium in 30 mins.

Thus, the contact time of 1h was selected in the batch experiments. The adsorption capacity of AgNPs-rGO composite was determined by using the following equation

$$q_e = (C_o - C_e)V/m \quad (1)$$

Where C_o is the initial concentration of MB (ppm), C_e is the concentration of MB at equilibrium (ppm), V is the total volume of the suspension (L), and m is the mass of adsorbent (g).

Kinetic studies were performed at a constant temperature of 35 °C and 120 rpm with 500 ppm of initial concentration of dye solutions at a predetermined time interval ranged from 0

Research Paper

© 2012 IJFANS. All Rights Reserved

to 60 min. The amount of adsorbed dye on adsorbents (q_t , mg/g) was calculated as follows

$$q_t = (C_0 - C_t)V/m \quad (2)$$

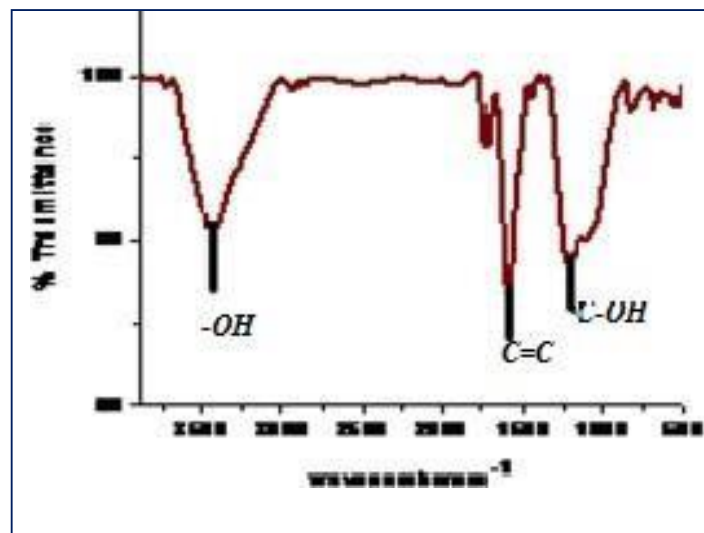
Where C_0 is the initial concentration of MB (ppm), C_t is the concentration of MB at time t (ppm), V is the total volume of the suspension (L), and m is the mass of adsorbent (g).

The thermodynamic studies of MB onto the AgNPs-rGO composite was carried at four different temperatures namely 25, 35 and 40 °C in aqueous medium.

RESULTS AND DISCUSSION

IR Spectroscopy

The functional groups present in the GO and AgNPs-rGO represented by FT-IR Spectroscopy.



The absorption peak at 1620 cm^{-1} can be ascribed to the skeletal vibrations of unoxidized graphitic domains (C=C) or contribution from the stretching deformation vibration of intercalated water [23,24]. In addition, the C-OH stretching peak at 1220 cm^{-1} and C=O stretching peak attributed to epoxy or alkoxy at 1060 cm^{-1} can also be observed. After adding leaf extract, during preparation of AgNPs-rGO composite, the C=O vibration band disappears, and the broad O-H and the C=O stretching bands remain. As the adsorption bands of oxygen functionalities disappear (C=O groups are considerably decreased) and only the peak at 1620 cm^{-1} remains, it demonstrates that rGO is achieved by addition of leaf extract

Research Paper
during the preparation of AgNPs-rGO composite..

XRD

The XRD patterns as shown in (Fig.3.2.a) were performed to analyze the crystalline structure. Comparison of the micrograph shows that before and after adsorption of metal ion on the surface of the material. The XRD data provided evidence of decrease in the peak intensity of 2θ values which shows that adsorption of metal ions on the surface of the adsorbent (Fig.3.2.b) indicate that decrease in the peak intensity values after adsorption of MB on the surface of the material.

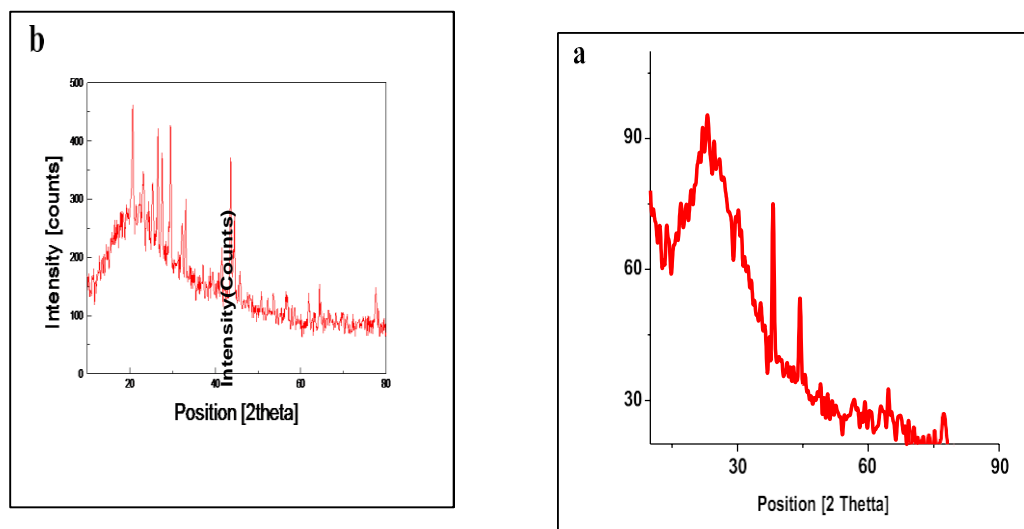


Fig.3.2: a and b XRD pattern of AgNPs-rGO before adsorption and after adsorption

Adsorption isotherm

To investigate the nature of interaction of AgNPs-rGO composite, rGO and AgNPs with MB dye molecule, adsorption isotherms experiments at different experimental conditions were carried out. The adsorption characteristics at equilibrium were analyzed by using Langmuir [42] and Freundlich [43] models and presented in Fig.3.3 & 3.4. Based on the adsorption data of the specimens shown in Table 3.1, the correlation coefficients of the isotherms are

Research Paper

relatively high(0.997 for AgNPs-rGO composite, 0.990 for rGO and 0.983 for AgNPs) which shows that the Langmuir isotherm model is better fit for describing the adsorption equilibrium of MB onto AgNPs-rGO composite, rGO and AgNPs with than Freundlich isotherm model. From that, the monolayer adsorption on structurally and energetically homogeneous active sites and predicts the monolayer coverage at the outer surface of the adsorbent [42].

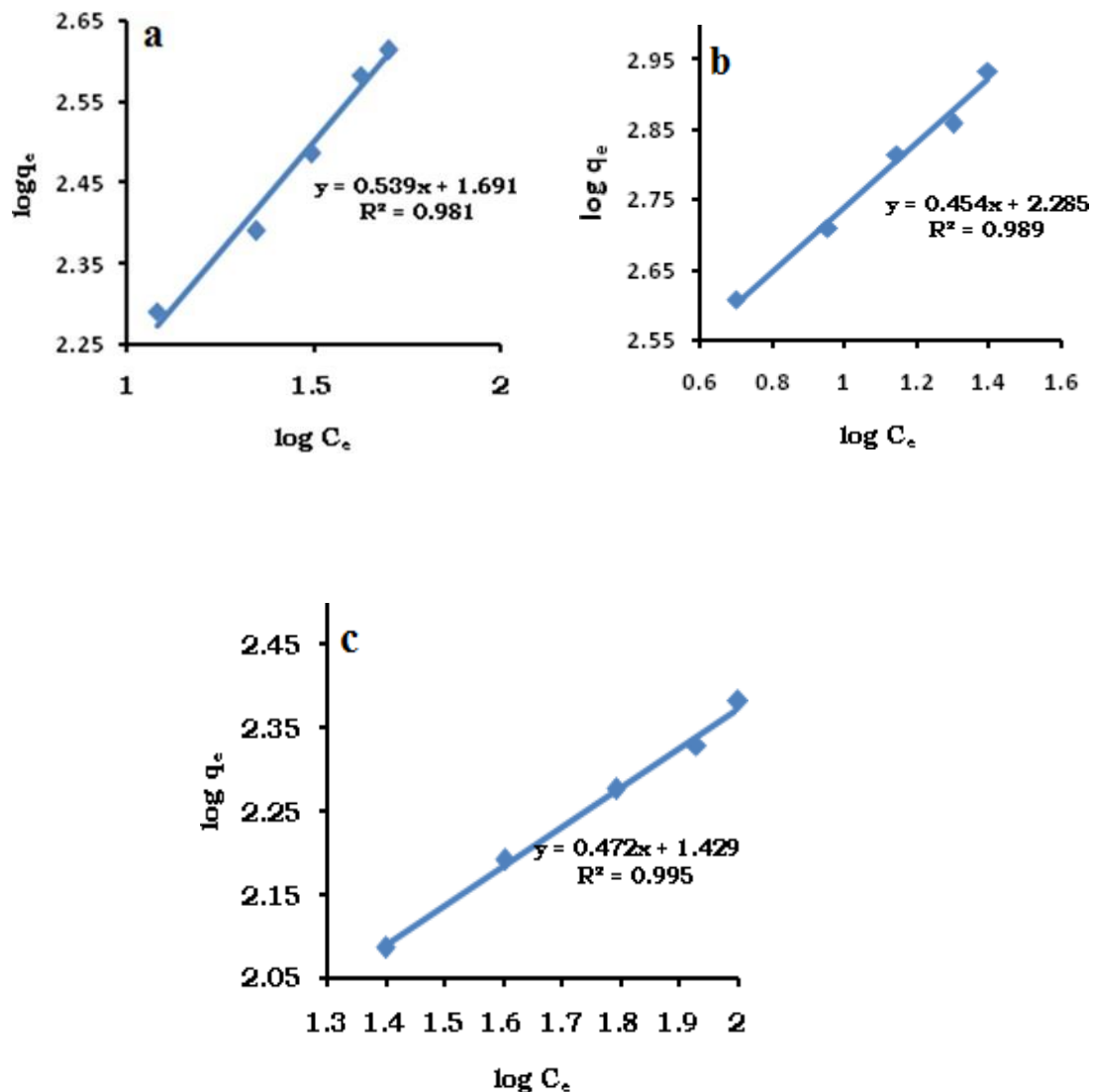
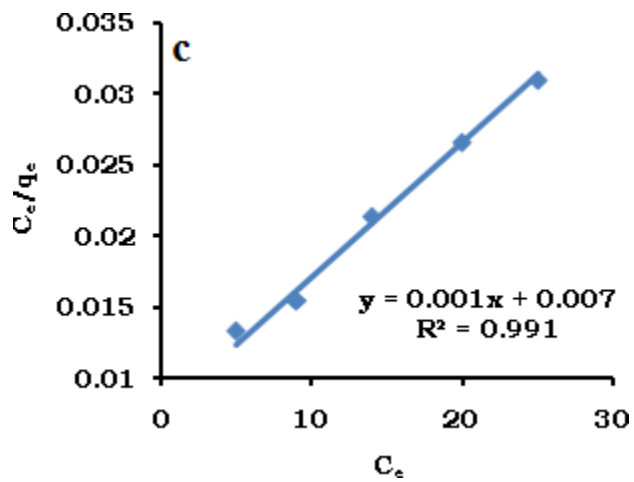
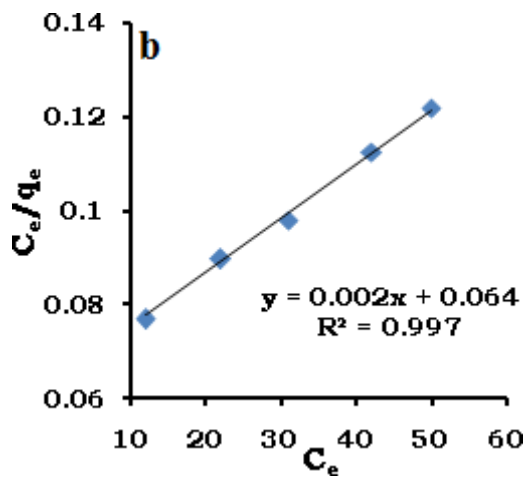
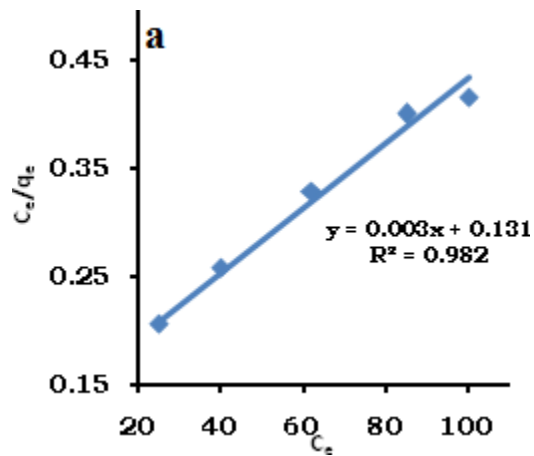


Fig.3.3.Freundlich adsorption Isotherm for the adsorption of MB by a) rGO b) AgNPs c) AgNPs-rGO

Research Paper



**Fig.3.4. Langmuirs adsorption Isotherm for the adsorption of MB by a) rGO
 b) AgNPs c) AgNPs-Rgo**

The R_L value indicates the shape of the isotherm to be either unfavorable ($R_L > 1$), linear ($R_L = 1$), favorable ($0 < R_L < 1$), or irreversible ($R_L = 0$). In the present investigation the R_L was found to be 0.0223, 0.0609 and 0.183 for AgNPs-rGO composite, rGO and AgNPs respectively indicating that the adsorption of MB is favorable.

Adsorbent	Langmuir				Freundlich		
	KL (1/mg)	qm (mg/g)	RL	R ²	KF	1/n	R
AgNPs-	0.163	877. 19	0.007	0.9 91	192.7 5	0. 22 5	0. 99 5
rGO AgNPs	0.031	500. 00	0.060 9	0.9 97	49.09 1	0. 15 6	0. 98 9
rGO	0.023	333. 33	0.116	0.9 82	26.85 3	0. 00 8	0. 98 1

3.2. Adsorption Kinetics

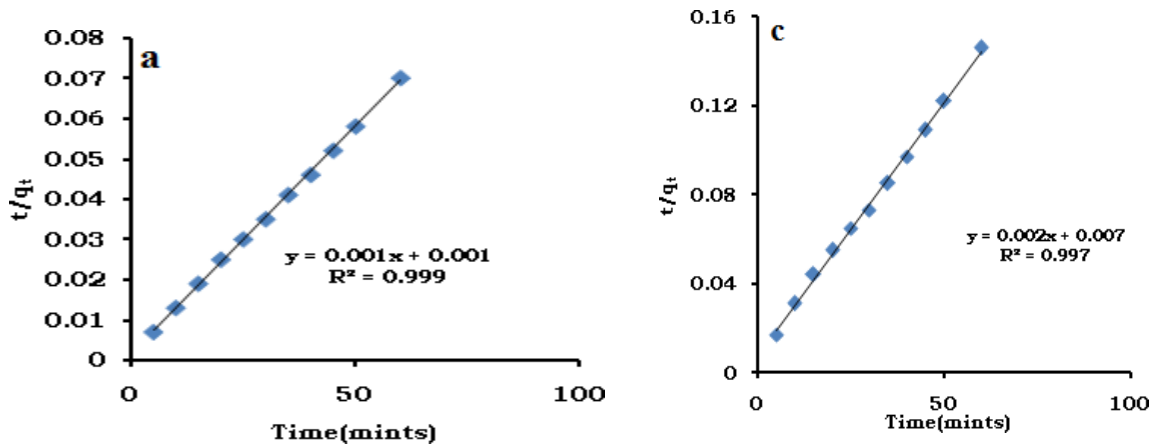
The adsorption Kinetics models were applied to investigate the adsorption rate and detailed mechanism of adsorption process. In general, the adsorption rate is considered as one of the most important factors for choosing an ideal adsorbent [44]. To study the adsorption mechanism well, pseudo first-order and pseudo second-order equations were used to applied. The Lagergren pseudo first-order kinetic model is expressed as [45]

$$\log (q_e - q_t) = \log q_e - k_1 t / 2.303 \quad (3)$$

Ho and McKay pseudo-second order kinetic model is expressed as [46]

$$t/q_t = 1/k_2 q_e^2 + t/q_e \quad (4)$$

where, q_e and q_t are the adsorption capacity of MB onto the synthesized material at equilibrium and at time t , respectively. k_1 (min^{-1}) and k_2 ($\text{g/mg}\cdot\text{min}$) also represent the rate constant of pseudo-first-order and pseudo-second-order kinetic models, respectively. The estimation of two models was performed by plotting the values of $\log (q_e - q_t)$ Vs t for pseudo-first-order model (fig. 3.6.), t/q_t Vs t for pseudo-second-order model.



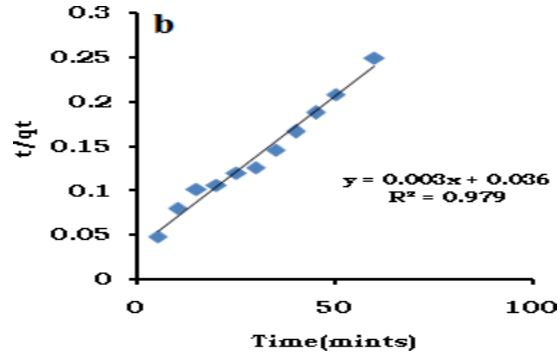
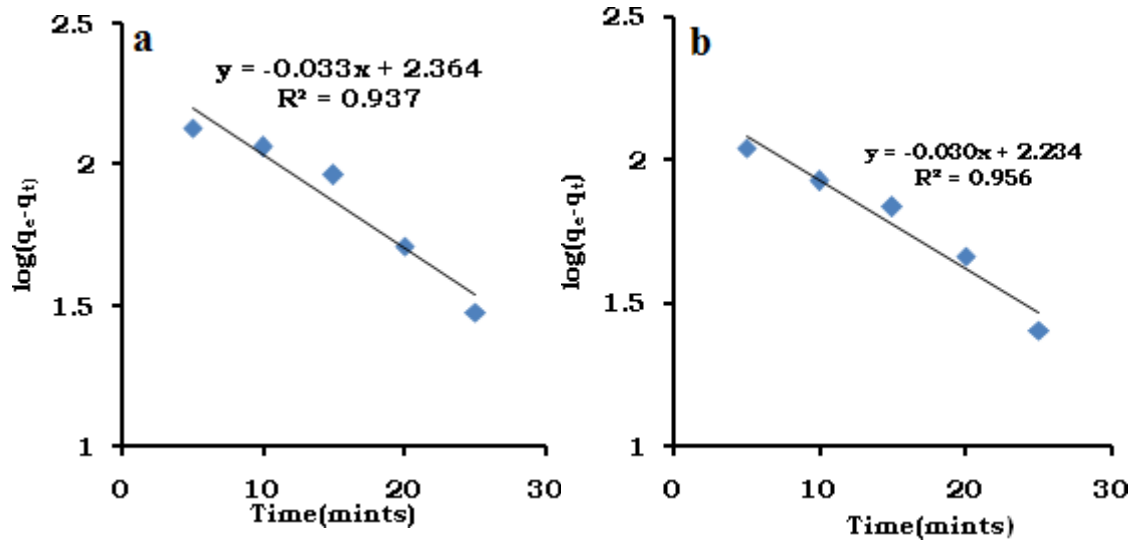


Fig.3.5. Pseudo Second order kinetics plot for the adsorption of MB by a) rGO b) AgNPs c) AgNPs-rGO



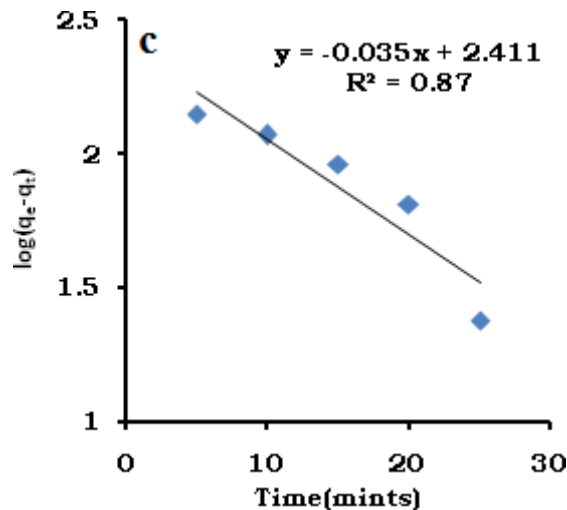


Fig.3.6. Pseudo First order kinetics plot for the adsorption of MB by a) rGO b) AgNPs c) AgNPs-rGO

The rate constants and q_e were obtained from the slopes and intercept of corresponding plots. All the corresponding kinetics parameters are listed in Table 3.2. According to our results the adsorption of dyes are best evaluated by pseudo-second-order kinetic model due to high correlation coefficient.

In addition, the calculated q_e values for pseudo-second-order kinetic model were best compliance with experimental q_e values thus also indicates that the overall rate of dyes adsorption processes follows pseudo second-order reaction mechanism. Since adsorption mechanism depends on the adsorbate and the adsorbent. Finally, the limiting rate in the adsorption of MB is a chemisorption mechanism through electrostatic attraction between active sites of adsorbent and dye molecules [47].

Intra particle diffusion model

It is vital to identify the steps involved during a solid liquid adsorption process. The adsorption process in porous solids could be described by three steps:(1) external mass transport of adsorbate from the bulk solution across the liquid film to the exterior surface of adsorbent (film diffusion or boundary layer diffusion or outer diffusion); (2) transport of adsorbate from the exterior surface of adsorbent to the pores or capillaries of the adsorbent

Research Paper

internal structure,(intraparticle diffusion or inner diffusion);(3) the adsorption of adsorbed onto the active sites of adsorbent in inner and outer surfaces. Generally, the rate of adsorption is controlled by boundary layer diffusion or intraparticle diffusion or both. To find out the actual rate controlling step involved in the MB adsorption process, we applied the Weber–Morris equation. Plots of q_t Vs $t^{1/2}$ are shown in Fig.3.7 , and the corresponding kinetic parameters are listed in Table 2. The intra- particle diffusion constant and the boundary layer thickness were calculated using the linear equation[48].

$$q_t = k_{id} t^{1/2} + C \tag{5}$$

where q_t is the amount of dye adsorbed onto the adsorbent at time t (mg/g), C is the boundary layer thickness, and k_{id} is the intra-particle diffusion rate constant(mg /gmin^{1/2})

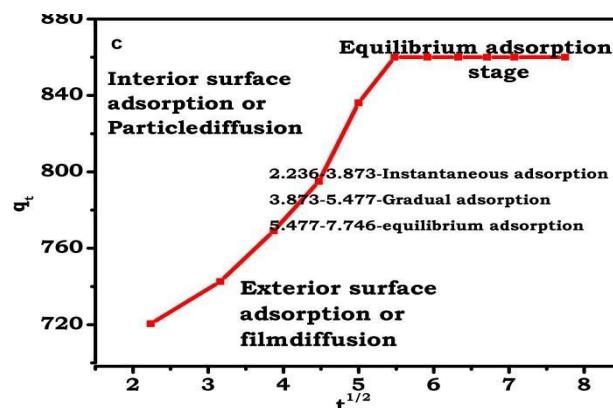
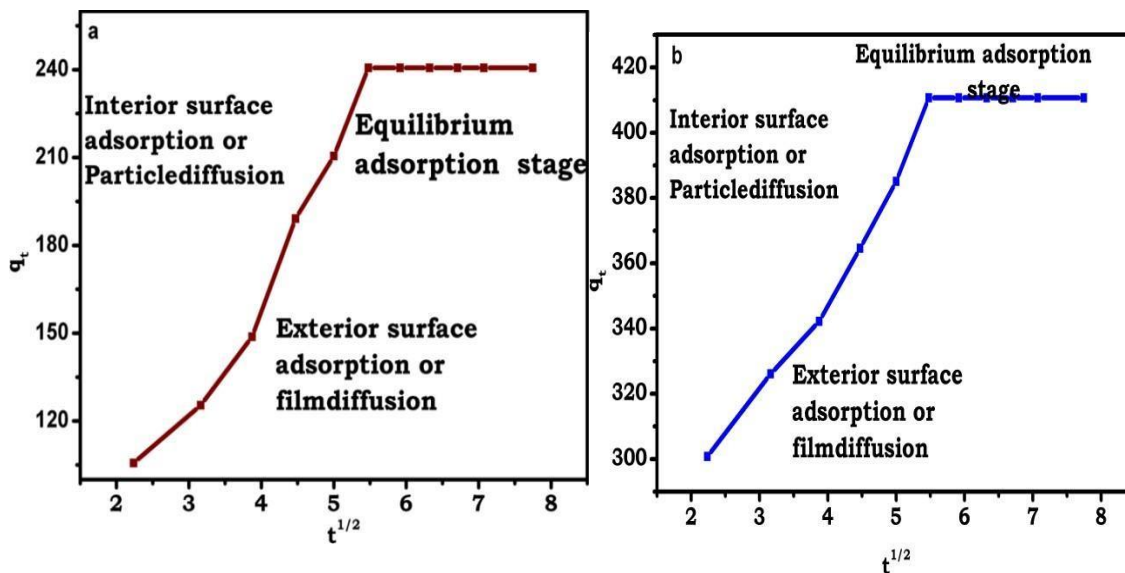


Fig.3.7. Webber - Morris plot for intraparticle diffusion a) rGO b) AgNPs c) AgNPs-rGO

It was also examined that the plots are not linear over the whole time range which means that the intraparticle diffusion is not the rate determining step the overall adsorption process may be jointly controlled by external mass transfer and intraparticle diffusion, and intraparticle diffusion played a predominant role in controlling the adsorption mechanism of the model dye onto [49]. The divergence of the plot from the linearity suggesting that the rate-limiting step must be controlled boundary layer diffusion because of the large intercepts of linear portion of the plots. The larger intercept the greater is the boundary layer effect and this means that the adsorption is more boundary layer controlled [50]. As can be observed from the Fig.7 the regression of q_t versus $t^{1/2}$ have multi-linear portions which indicates that the three stages control the adsorption process. The instantaneous adsorption was occurred in the initial linear portion resulting from the diffusion of dye through the solution to the external surface of adsorbent. The gradual adsorption stage was occurred in second linear portion, corresponding to intraparticle diffusion of dye molecules through the pores of adsorbent. The equilibrium adsorption was occurred in the third stage where the intraparticle diffusion starts to slow down due to the extremely low adsorbate left in aqueous solution and the decrease of adsorption sites [51]

SEM:

Further, SEM images of before and after adsorption of MB by AgNPs, rGO and AgNPs-rGO as shown in Fig 3.11. SEM images of before adsorption reveals that the rGO sheets decorated uniformly by AgNPs.

After adsorption, it is clearly seen that the size and structure of synthesized materials was changed. There are some cracks and irregularities structure is formed on the surface due to adsorption of MB molecules in the interior portion of the materials.

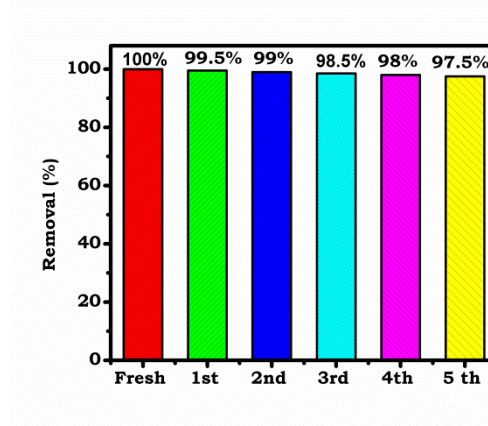
Reusability

As is well known, an efficient adsorbent should exhibit not only high adsorption capacity but also good stability and reusability in order to reduce the overall cost and also is vital for

Research Paper

© 2012 IJFANS. All Rights Reserved

water treatment application. Thus, the regeneration performance of AgNPs-rGO was analyzed are shown in Fig.3.12. By comparing the removal efficiency of dyes on the regenerated and fresh adsorbent, it can be concluded that more than 90% of MB can be removed from the solution by the regenerated adsorbent even after five cycles.



More importantly, desorption of the cationic MB dye was demonstrated simply by washing with deionized water. Therefore the AgNPs-rGO can be repeatedly used as a promising adsorbent for removal of cationic dyes from aqueous solution.

Conclusion

In conclusion, AgNPs-rGO have been successfully synthesized through simple green method which could be used as an effective, non hazards and recyclable adsorbent for water treatment application. The green synthesized AgNPs- rGO reveals superior performance for the fast and effective removal of MB from aqueous solution, with a maximum adsorption capacity of 860.07mg g⁻¹ within 30 min at natural pH and room temperature than other adsorbents reported so far. Thus, the AgNPs-rGO nanocomposite can be considered as a very effective adsorbent for removal of dye molecules from wastewater due to the strikingAgatures like high adsorption capacities, separation convenience and facile preparation process from nontoxic materials.

Environment pollution is a global problem since it is responsible for the continuous deterioration of the beauty of nature. Almost every aspect of modern life style attacks the environment and imposes potential health risks. The air we breathe, the water we drink and the places where we dwell are contaminated with toxic substances. Water is one of the prime

Research Paper

© 2012 IJFANS. All Rights Reserved

necessities of life. It is nature's most wonderful, abundant and useful compound, which is highly essential for the lives of human beings, animals and plants. Its role in the area of industries is also significant. The removal of hazardous substance from waste streams is really a significant environmental challenge. The study of the distribution of heavy metal ions and dye between solid phase and liquid phase has great eco-toxicological significance. Solid surfaces are sites of adsorption phenomenon, which is the most promising technique suitable for the removal of metal ions and dye from water. Recognizing the economic drawbacks (high capital and regeneration costs) associated with the use of commercial by activated carbons and ion exchange resins, the present study aimed to prepare some suitable and cost-effective green synthesis of nano composite adsorbents and to test their potential to abate metal ions and dye from aqueous solution. The work reported in this thesis deals with the investigation on the equilibrium, kinetic and thermodynamic aspects of the adsorption of metal ions such as Hg(II), Ag (II), Cd(II) and Pb(II) and dye namely methylene blue dye onto the four chosen nano composite adsorbents viz. **AgNPs- rGO**, **nAg-MFR**, **MWCNTs-PFR** and **betaCD-PFCR**. The different parameters pertaining to the adsorption at equilibrium are determined in order to establish the behavior of the adsorption process. It also describes the different technologies that have already been employed for the purpose of pretreatment of wastewater as well as the removal of dye and heavy metal ions. Merits and demerits of these technologies have also been explained.

REFERENCES

1. N. Narendran, A review on environmental problem due to water pollution, (2015) *Int. J. Sci. Eng. Res.*, 3, 43-45.
2. W. Larry, A billion people worldwide lack safe drinking water, (2006) *World water day*.
3. F. N Chaudhry, M. F Malik, Factors affecting water pollution: a review, (2017) *J. Ecosyst. Ecography*, 7, 111-118.
4. A. Florescu, R. E Ionete, C. Sandru, A. Iordache, M. Culea, The influence of pollution monitoring parameters in characterizing the surface water quality from Romania southern area, (2010) *Rom. Journ. Phys.*, 56, 7-8.

Research Paper

5. A. B. Bhuiyan, M. B. Mokhtar, M. E. Toriman, M. B. Gasim, G. C. Ta, R. Elfithri, M. R. Razman, The environmental risk and water pollution: a review from the river basins around the world, **(2013)** *Am. Eur. J. Sus. Agri.*, 7, 126- 136.
6. C. Claudia, **(2016)** *Clean Water Act Section United States*.
7. A. Bergman, J. Heindel, S. Jobling, K. A. Kidd, R. T. Zoeller, State of the science of endocrine disrupting chemicals, **(2013)** *World Health Organization (WHO) and United Nations Environment Programme (UNEP)*,505031.
8. B. Keul, L. Momeu, C. Craciunas, C. Dobrota, S. Cuna, G. Balas, Physico-chemical and biological studies on water, **(2012)** *J. Environ. Manage.*, 95, 234-242.
9. G. M. Dias Ferreira, M. C. Hespanhol, J. de Paula Rezende, A. C. Santos Pires, L. V. Alves Gurgel, L. H. Mendes da Silva, Adsorption of red azo dyes on multi-walled carbon nanotubes and activated carbon: A thermodynamic study, **(2017)** *Colloids Surf., A: Physicochem. Eng. Aspects*, 529, 531-540.
10. B. Satilmis, P.M. Budd, Selective dye adsorption by chemically-modified and thermally-treated polymers of intrinsic microporosity, **(2017)** *J. Colloid Interface Sci.*, 492, 81-91.
11. V.K. Gupta, R. Kumar, A. Nayak, T.A. Saleh, M.A. Barakat, Adsorptive removal of dyes from aqueous solution onto carbon nanotubes: A review, **(2013)** *Adv. Colloid Interface Sci.*, 193, 24-34.
12. E. Khalid, L. Abderrahmane, A. Abdellah, A. Mohamed, Removal of methyl violet from aqueous solution using a stevensite-rich clay from Morocco, **(2011)** *Appl. Clay Sci.*, 54, 90–6.
13. M. Pateiromoure, M. Ariasestévez, J. Simalgándara, Critical review on the environmental fate of quaternary ammonium herbicides in soils devoted to vineyards, **(2013)** *Environ. Sci. Technol.*, 47, 4984-4998.
14. X. Wang, X.J. Li, Z. Li, Y.D. Zhang, Y. Bai, H.W. Liu, Online coupling of in-tube solid-phase microextraction with direct analysis in real time mass spectrometry for rapid determination of triazine herbicides in water using carbon-nanotubes-incorporated polymer monolith, **(2014)** *Anal. Chem.*, 86, 4739-4747.

Research Paper

© 2012 IJFANS. All Rights Reserved

15. S. Siva, S. Sudharsan, R. Sayee Kannan, Selective Co (II) removal from aqueous media by immobilizing silver nanoparticles within a polymer matrix through formaldehyde cross linking agent, **(2015)** *RSC Adv.*, 5, 23340– 23349.
16. S. Siva, S. M. Sameem, S. Sudharsan and R. Sayee Kannan, Synthesis, characterization and application of zero-valent silver nano adsorbents, **(2013)** *Ind. Eng. Chem. Res.*, 2, 8023–8037.
17. G. Dursun, H. Cicek, A. Y. Dursun, Adsorption of phenol from aqueous solution by using carbonized beet pulp, **(2005)** *J. Hazard. Mater. B*, 125,175–182.
18. M. Wawrzekiewicz, M. Wisniewska, V.M. Gunko, V.I. Zarko, Adsorptive removal of acid, reactive and direct dyes from aqueous solutions and wastewater using mixed silica-alumina oxide, **(2015)** *Powder Technol.*,278,306-315.
19. J. Goscianska, N. A. Fathy, R. M. M. Aboelenin, Adsorption of solophenyl red 3BL polyazo dye onto amine-functionalized mesoporous carbons, **(2017)** *J. Colloid Interface Sci.*, 505, 593-604.
20. B. Vellaichamy, P. Periakaruppan, Ag-Nanoshells catalyzed dedying of industrial effluents, **(2016)** *RSC Adv.*, 6, 31653–31660.
21. R. Sanghi, P. Verma, Decolorisation of aqueous dye solutions by low-cost adsorbents: a review, **(2013)** *Color. Technol.*, 129, 85–108.
22. M. Rafatullah, O. Sulaiman, R. Hashim, A. Ahmad, Adsorption of methylene blue on low-cost adsorbents: a review, **(2010)** *J. Hazard. Mater.*,177, 70–80.
23. Y. Ge, Y. Xiang, Y. Hu, M. Ji, G. Song, Preparation of Zn-TiO₂/RH/Fe₃O₄ compositematerial and its photocatalytic degradation for the dyes in wastewater, **(2016)** *Desalin. Water Treat.*, 57, 9837–9844.
24. A. K. Verma, R. R. Dash, P. Bhunia, A review on chemical coagulation/ flocculation technologies for removal of colour from textile wastewaters, **(2012)** *J. Environ. Manage.*, 93, 154-168.
25. A. Baban, A.Yediler, N. K. Ciliz, Integrated water management and CP implementation for wool and textile blend processes. **(2010)** *CLEAN–Soil, Air, Water*, 38, 84-90.